Genetic deletion of calpain-1 and pharmacological inhibition of calpain activity improve red blood cell morphology and reduce sickling in humanized mouse model of sickle cell disease

A thesis submitted by

Aliya Butabayeva

In partial fulfillment of the requirement for the degree of

Master of Science

In

Pharmacology and Drug Development

Tufts University

Sackler School of Graduate Biomedical Science

May 2019

Adviser: Athar Chishti, PhD

Abstract

Sickle cell disease (SCD) is a genetic hematological disorder caused by inheriting two copies of mutated hemoglobin S gene (HbS) located in codon 6 of globin gene causing the insertion of valine in place of glutamic acid. The mutated hemoglobin undergoes increased polymerization in deoxygenated state, and changes erythrocyte properties generating sickle shape. It has significantly short life span leading to anemia, vaso-occlusive events, and organ impairment. In this study, we investigated the remodeling effects of calpain-1 (CAPN1) on red blood cell (RBC) membrane using calpain-1 null mouse model of sickle cell disease (SSCKO). CAPN1 associates with RBCs membrane and cleaves membrane proteins at high calcium concentration. Patients with SCD have a high level of calcium in erythrocytes that activates calpain-1 and changes its morphology to sickle shape. The genotype of AA, SS and SSCKO was confirmed by PCR. Blood samples collected from the facial vein of AA, SS and SSCKO mice in Heparin coated tube were washed with RPMI and exposed under normoxia (20%-O_2, T-37^oC) and hypoxia (3%-O_2, 5%-CO_2, T-37^oC) for different time intervals and visualized under 60X oil objective by microscopy. No significant difference between the morphology of SS and SSCKO erythrocytes was observed under normoxia condition; however, SSCKO erythrocytes showed significantly higher resistance to hypoxia-induced sickling as compared to SS upon 3-hour hypoxia. The calpain activity measurements showed that SS erythrocytes contain higher activity then SSCKO mice. However, treatment with a pan-calpain inhibitor significantly reduced calpain activity in SS compared to vehicle treated control cells. Moreover, treatment of cells with MDL28170 showed significant reduction in the number of sickle erythrocytes and reticulocytes upon

3-hour exposure to hypoxia. Together, these findings suggest that both calpain-1 and calpain-2 serve as potential therapeutic targets for exerting anti-sickling effects on erythrocytes and reticulocytes under hypoxic conditions.

Acknowledgments

I would like to thank Tufts University for giving me an opportunity to be a part of the Tufts community and experience a wonderful academic environment. I am grateful to all professors for the amazing lectures, for sharing their knowledge and professional experience. It was a great pleasure and a wonderful experience for me to work under the guidance of Dr. Chishti. I want to thank Dr. Chishti for his advice, guidance, providing me with invaluable information, helping me to build my research capacity and extending my knowledge in science. He is a true expert! I was always inspired by his enthusiasm and ideas. I have known him as an open-minded person, always being available, supportive, encouraging me doing better. I am fortunate to learn a lot from my amazing colleagues in the laboratory. I want to thank everyone in the laboratory, Donna-Marie Mironchuk, Toshihiko Hanada, Daniel Fritz, and Christopher Schwake, for always being helpful, sharing their experience, for creating friendly and right environment. I also want to thank Farha Mithila for her excellent mentorship. I cannot thank her enough for everything, and providing an opportunity to gain high quality professional knowledge. I express my gratitude to Farha for her fruitful work and wish her further prosperity and many professional victories!

Table of Content

List of Figures:

List of Abbreviations:

(CAPN) Calpain
(CKO) Calpain-1 Knockout
(dd) Distilled water
(DMSO) Dimethyl Sulfoxide
(DNA) Deoxyribonucleic Acid
(DPBS) Dulbecco's Phosphate Buffered Saline
(EDTA) Ethylenediaminetetraacetic Acid
(ESL) Chemiluminescence
(HbS) Hemoglobin S
(PCR) Polymerase Chain Reaction
(RBC) Red Blood Cell
(SCD) Sickle Cell Disease
(SDS-PAGE) Polyacrylamide Gel Electrophoresis
(SSCKO) Calpain-1 Knockout Sickle Mice
(SS) Homozygous Sickle Cell Disease
(TBE) Tris-Borate-EDTA
(TBST) Tris-Buffered Saline +Tween 20
(UV) Ultraviolet
(WT) Wildtype

Chapter 1: Introduction

Sickle cell disease (SCD), a disorder manifested under conditions of hypoxia (28), is caused by a genetic mutation of the beta globin chain and changing its conformation to generate sickle hemoglobin (HbS) (9, 30, 17). The main pathophysiological factor of the disease is red blood cell (RBC) sickling under hypoxia conditions causing vaso-occlusive events and organ damage in homozygous sickle cell (SS) disease (1, 17, 19, 28). Every year more than 330, 000 newborns are affected by the disease in worldwide (32), particularly in sub-Saharan Africa and southern Asia (6). Moreover, it is a leading cause of morbidity in children between 1 and 4 years in the USA and Western Europe (9). The treatment options are limited till today, and only hydroxyurea is currently approved for SCD (9).

Our laboratory has been investigating the role of calpain-1 in red blood cells with therapeutic implications for the SCD (22,23). Calpains (CAPNs) are calcium activated cytosolic proteases regulated by Ca^{2+} (40, 41). CAPN1 plays a functional role in the regulation of calcium pump as well in the structural and functional stability of the RBC membrane (34) There are 15 calpain isoforms that have been identified in the human genome; human erythrocytes have only CAPN1 or μ-calpain (22, 29) and it is regulated by activator protein and endogenous inhibitor calpastatin. CAPN1 is activated in micromolar calcium, whereas CAPN2 or m-calpain is activated at millimolar calcium concentration (7, 10, 22). It has been reported that Hb SS red blood cells contain approximately eight times higher calcium concentration compared to normal RBCs, and their permeability to calcium is enhanced upon deoxygenation thus damaging the membrane of homozygous (SS) erythrocytes (13) causing its sickling. The calpain and

capastatin system is also dysregulated upon enhanced intracellular calcium concentration in SCD. Activated CAPN1 in RBCs cleaves membrane proteins causing band 3 and other structural protein degradation under elevated intracellular calcium (23, 34, 41). Our laboratory previously showed the improved morphology of red blood cells in calpain-1 knockout (KO) mouse model compared to WT (22), and *in vivo* treatment with inhibitor calpain-1, BDA-410, showed positive results in a mouse model of mild SCD (23).

Calpains play a critical role in controlling cellular homeostasis, cytoskeleton reorganization, apoptosis, neuronal biogenesis (15, 22,29). Calpain inhibitors have been used in a variety studies and shown protective effects in the neurodegenerative diseases, cardiovascular disorder, myopathies, cataracts, infectious diseases, and cancer research (29, 33, 37, 25, 23, 18,11, 5).

The overall goal of this project is to study the functional effects of calpain-1 in SCD using the calpain-1 null mouse model of SCD generated by the Chishti laboratory by crossing CKO mice with Townes SS mice. Our findings suggest that genetic deletion of calpain-1 and pharmacological inhibition calpain activity improve red blood cell properties by reducing sickling under hypoxic conditions.

Chapter 2: Methods

2.1 Mouse genotyping and PCR

2.1.1 Animals for *ex vivo* testing

The 5- and 10-months old age-matched homozygous male mice were used for all experiments. Three mice per group were tested in three independent experiments. Humanized (AA) mice were used as a control. Townes sickle (SS) mice were obtained from the Jackson Laboratory, Humanized calpain-1 knockout sickle (SSCKO) mice were generated in our laboratory by backcrossing Townes sickle (SS) mice with calpain-1 knockout with C57BL/6 (CKO) background (15).

2.1.2 Husbandry and housing conditions

All mice were bred and housed at Tufts University Animal Facilities with 24 h access to food and water. All animal protocols used in this study are approved by the IACUC (Institutional Animal Care and Use Committee) of Tufts University and performed in accordance with guidelines of the IACUC.

2.1.3 Genomic DNA extraction from mouse tails

Genomic DNA was extracted from mouse tails of AA, SS and SSCKO models. A stock solution was prepared using Direct PCR Reagent and Proteinase K (250 µL reagent used per 0.5 cm tail, 30 µL Proteinase K per 1.0 mL reagent) and added 150 µL of stock per tail. Then, the samples were incubated in each vial at 55^{o}C overnight and increased at 85^{o}C for 45 minutes the following day. The samples were centrifuged for 1.0 min, and supernatant containing DNA was carefully collected and stored at -80^{o}C.

2.1.4 Polymerase chain reaction (PCR)

The following primers were used for Calpain-1 alleles, CAL1F (5´-TGCACTCTAGTTCTGAGGCT-3´), CAL65 (5´AGAGTGCACGAACACCA GCTT-3´) and for the CKO allele, NEO-RO-calpain ((5'-TTAAGGGCCAGCTCATTCCT-3') and CAL1F primers were used. For common α, primer sequence was (5' TCTATGCACATCAATTAGCAGAGGC 3'); human/mutant α reverse was (5' TCCTGCAGGGTGAGGAAGGAAGG 3') and mouse/WT α globin reverse primer sequence was (5' CCCCAAGGCACTCCAGGGACATAG 3'); Primer sequence for WT β reverse was (5' ATGTCAGAAGCAAATGTGA GGAGCA 3'), HbA reverse was (5' GTTTAGCCAGGGACCGTTTCAG 3'), HbS reverse was (5'AATTCTGGCTTATGGGAGGCAAG 3') and β common forward was (5' TTGAGCAATGTGGACAGGAAGG 3').

The PCR was performed using a touchdown protocol and analyzed by 1.2% agarose gel electrophoresis in 1X TBE at 60V for 5 minutes. The voltage was then increased to 80V and samples were run for another 30 minutes and visualized under UV (Bio-Rad). The 100 bp ladder was used as a size marker.

2.2 Normoxia and hypoxia measurements *in vitro*

2.2.1 Blood collection and red blood cell (RBC) isolation

Blood was collected from the facial vein of three different groups of mice (AA, SS and SSCKO) by inhalation of isoflurane. Approximately 100µL blood was collected into heparin tubes and transferred into a 1.5ml Eppendorf tube. The whole blood was washed three times in RPMI (Medium 1640 1X) containing 10 mM HEPES, pH 7.4,

buffer and samples were centrifuged at 1,000 rpm for 5 min, at 4ºC. The supernatants were removed after each wash and the RBC pellet was saved each time for analysis.

2.2.2 Cell exposure under normoxia and hypoxia conditions

The RBC pellets from AA, SS and SSCKO erythrocytes were divided into three equal parts. The first part was smeared and fixed with 100% absolute methanol. This step was considered as an initial blood sample or untreated sample. The RPMI 1640 (1X) medium containing 10 mM HEPES, pH 7.4, was added to the rest of samples in the 96 well-plate with final concentration of 50µL; then one part of the samples was exposed in normoxia (20% O_2, T-37ºC) using normal incubator and the other part was exposed in hypoxia (3% O_2, 5% CO_2, T-37ºC) using a hypoxia chamber for 1, 2, and 3 hours under the same conditions. Before touching the hypoxia chamber, precautions were taken by spraying plates with EtOH to avoid any contamination.

2.2.3 Blood smears and staining with Wright-Giemsa

The samples were taken out at desired time points after normoxia and hypoxia exposure, and immediately smeared with equal parts of packed RBC (2 µL) using single frosted microscope glass slides. Each slide was fixed with 100% absolute Methanol for 30 seconds and left to dry overnight. Then, the slides were stained with Wright-Giemsa Dye (Sigma) for 30 seconds and washed immediately after dye with distilled (dd) water for 10 minutes and air dried at least 40 minutes.

2.2.4 Microscopy

The blood smears were visualized under 60X objective using a Nikon immersion oil microscope. Images were analyzed for erythrocyte shape changes from random fields of captured images, 10 images were acquired from 3 different slides. The total and sickle erythrocytes and reticulocytes numbers were counted manually, and the percentage of sickle RBCs and reticulocytes were calculated using the Microsoft Excel.

2.3 Treatment with calpain inhibitor

2.3.1 Preparation of MDL-28170 inhibitor

MDL 28170, a pan-calpain inhibitor with molecular weight 382.45 was purchased from APExBIO company, and made 0.1 M stock solution with DMSO (10 mg of inhibitor was dissolved in 261 µL DMSO) and stored in -20ºC. Two different final DMSO concentrations were selected for the working solutions at 0.1% and 0.5%, and two different inhibitor concentrations at 100 µM and 500 µM were used, respectively.

2.3.2 MDL-28170 treatment

The final volume of the media was 300 µL (v/v) containing RPMI 1640 (1X) 10 mM HEPES, pH 7.4, MDL28170 at 100 µM and 500 µM concentration and RBC pellet (10 µL) of sickle mouse model (SS), All reagents were mixed together in a 96-well plate and exposed for 3-hours under hypoxia (3% O_2, 5% CO_2, T-37ºC). The first part of the sample was incubated without inhibitor, which was considered as untreated, the other part was incubated only with DMSO, and the final part was treated with MDL28170.

Immediately after incubation, each sample was smeared, stained, and visualized under 60X objective using a Nikon immersion oil microscope.

2.4 Calpain-Glo Protease Assay

2.4.1 RBC ghosts preparation

Whole blood from three different groups of mice was collected from the mouse facial vein. The blood was then washed three times in RPMI 1640 (1X) at 1,000 rpm for 5 minutes at 4ºC. The supernatant was removed (plasma and platelets) after each time of washing. Approximately 700 µL of ice cold 5P8 lysis buffer (5 mM sodium phosphate buffer, pH 8.0 from 0.1 M in stock solution and 1.0 mM EDTA, pH 8.0 from 0.5 M stock) was added, vortexed, and incubated on ice for 10 minutes. After incubation, the samples were centrifuged at 12,000 rpm for 10 min in 4ºC. White fluffy pellet was formed. The supernatant was removed, and pellet was washed with 5P8 at least three times until the pellets became almost white. The supernatant samples were removed after the last wash, and 5µL of 5P8 was added to the samples for storage at -80ºC for later use.

2.4.2 Calpain activity measurements *in vitro*

The calpain activity assay was performed using the commercially available substrate, Suc – LLVY aminoluciferin (Promega). White-walled 96 well plates were selected for this assay since the use of black plates reduced sensitivity as measured by RLU. The Promega Calpain Glo Assay reagent was prepared and saved in aliquots at -20ºC for further use. The calpain assay was performed by following the protocol of homogeneous "add-mix-read". The equal amount of RBC ghosts from each group of AA, SS and SSCKO mice

were resuspended in the lysis buffer (5P8) and mixed with the Calpain Glo reagent in a ratio of 1:1 into 96-well white plates with a final volume of 50 µL of blank, control, and sample. The reaction was initiated by adding of 2 mM $CaCl_2$ (from 50 mM stock). After addition of CAPN Glo reagent, the samples were stored in dark to avoid exposure to light. The protein concentration of RBC ghosts of each group was measured with the Bradford Bio-Rad assay in order to normalize the amount of protein in each sample. The luminescence (or RLU) was measured using the plate reader for 45 min in 5 minutes interval (TECAN SpectraFluor Plus Luminometer). Generally, the 15 minutes reading gave the best activity measurements.

2.4.3 Measurement of MDL 28170 inhibitory effects *in vitro*

The RBCs of sickle (SS) mice were treated with MDL inhibitor at two different concentrations, 100 µM and 500 µM dissolved in two different DMSO concentrations, 0.1% and 0.5%, respectively. The RBCs were lysed by re-suspending in the lysis buffer containing 5P8, then Calpain Glo reagent was added in a ratio of 1:1. Finally, 2 mM $CaCl_2$ from 50 mM in stock was added to initiate the reaction (ttotal volume =100 µl), mixed, and luminescence was recorded in 5 minutes interval for 45 min as described above.

2.5 Protein quantification using Bradford assay

2.5.1 Standard protocol for microtiter plates

Protein assay dye reagent (Bio-Red) was prepared by diluting one part of Dye reagent concentrate with four parts of distilled water. Then, seven serial dilutions of a protein standard were prepared (125 µg/ml BSA used for this assay). To prepare samples, 10 µl of each standard and sample solution were added into the 96-well plates, followed by the addition of 200 µL of diluted reagent into each well. The samples were incubated at room temperature for 5 min and absorbance was measured at 595 nm using microplate reader (VersaMax). Finally, a standard curve was generated for the protein assay with bovine serum albumin, and all protein concentrations from three different groups of AA, SS and SSCKO were calculated based on the standard curve.

2.6 Polyacrylamide gel electrophoresis and Western blot analysis

2.6.1 Preparation cell lysates

For Western blot analysis, intact RBCs were washed three times with DPBS at 1,000 rpm and 4^{o}C for 5 min. The RBC pellet was lysed in the ice cold 5P8 lysis buffer containing 5.0 mM sodium phosphate buffer, pH 8.0 and 1.0 mM EDTA, pH 8. The cell lysate was vortexed and incubated on ice for 10 min. After incubation, the samples were centrifuged at 12,000 rpm for 10 min in 4^{o}C. The supernatant was aspirated completely and this step was repeated 4 times. The cell lysate was stored at -80^{o}C. The protein concentration in each sample was measured using the Bradford protein assay as described above. An aliquot of RBC lysate was solubilized with 2X SDS sample buffer containing 0.5 M Tris-HCl, pH 6.8, 20% Glycerol, 10% (w/v) SDS, ddH_2O, 0.1% Bromophenol blue,

and 2-ME (15 µL). The protein samples of three groups of mice were loaded without heating since the protein samples of SS mouse model were found to be degraded after 5 min of heating at 90^{o}C.

2.6.2 Protein separation by SDS PAGE and transblotting to the nitrocellulose membrane

Protein samples were separated on 10% SDS-polyacrylamide gel (30% Acrylamide, 1.5M Tris-HCl, pH 8.8, 10% SDS, 10% APS, dd H_2O, 16 µL TEMED) and 4% stacking gel (30% Acrylamide, 0.5M Tris pH 6.8, 10% SDS, 10% APS, TEMED 10µL) by electrophoresis at 100V, Protein samples at 20 µg were loaded into each lane and 10-250 kDa protein ladder (ThermoFisher Scientific, Lithuania) was used to estimate the size of protein band. After electrophoresis, the proteins were transferred to the nitrocellulose membranes at 200 mA.

2.6.3 Incubation of Western blots with primary and secondary antibodies

The nitrocellulose membrane was blocked in the Tris buffered saline (TBS) containing 0,1% Tween-20 (TBST) and 5% dried milk for 2 hours at room temperature on a shaker. The membrane was then incubated with the primary monoclonal calpain-1 antibody (MAB3104, Chemicon International, Temecula, CA) diluted 1,000-fold in TBST for 1.0 hour at room temperature. After removal of the primary antibody, the membrane was washed with TBST three times with 5 min interval. The membrane was incubated with the secondary HRP-conjugated anti-mouse antibody at 5,000 dilutions for 1.0 hour at room temperature. After washing 3 times with TBST, the blots were

developed with chemiluminescence (ESL) substrate (Thermofisher scientific) solution for 1.0 min and gel images were captured on Imaging System (Bio-Rad).

2.7 Statistical analysis

Statistical analysis was performed using the GraphPad Prism. One-way and Two-way ANOVA with Tukey's multiple comparison test to compare values amongst three different groups. A p-value less than 0.05 was considered to be significant. All data were expressed as mean ± S.D. Error bars were generated on the basis of calculated SD values.

Chapter 3: Results

3.1 PCR genotyping based confirmation of calpain-1 null humanized mouse model of Sickle Cell Disease (SCD).

We have used three different humanized mouse models in this study to demonstrate the absence of mouse globin, presence of human alpha and human beta sickle globin, and calpain-1 knock out allele. The AA mouse model was used as a control group and carries normal human α and β hemoglobin in the presence of wild type calpain-1 gene. Next, the SS or Townes sickle mouse model contains normal human α and mutated β globin or hemoglobin S in the presence of wild type calpain-1 gene. The third group includes SSCKO mouse model that contains human α, mutated human β globin or Hb S from SS Townes mouse with the absence of calpain-1 gene. PCR confirmation of respective genotypes of AA, SS and SSCKO are shown in Figure 3.1. Data shown in Figure 3.1A (Lanes 1,2,3) confirmed AA genotype containing both normal human α and β globin bands at 320 bp, whereas lanes 4-9 demonstrate SS genotype band at 250 bp. Similarly, data shown in Figure 3.1B (lanes 2-3) confirm heterozygous AS mouse genotype bands between 250 and 320 bp; Figure 3.1C (lanes 7-8) indicate the presence of WT/CKO allele at 432 pb; Figure 3.1D demonstrates the presence of human α globin band at 330 pb; panel 1E (Lanes 2,3,5, and 6) demonstrates the presence of calpain-1 band at 650 bp; panel 1F (Lanes 4,7, and 8) confirms the absence of calpain-1 gene with the Neo Cassette in SSCKO mouse model band at 415 pb;

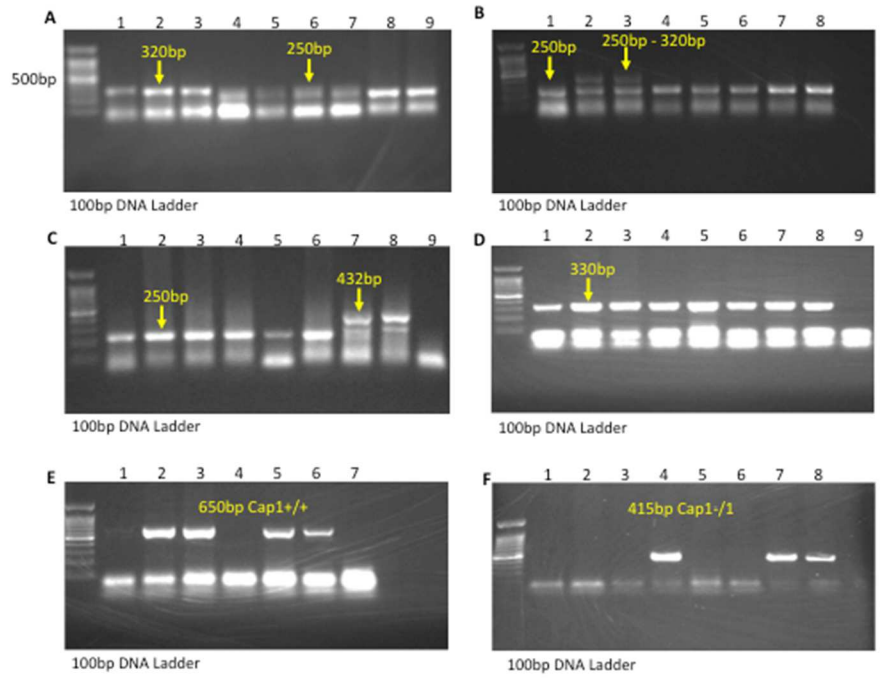

Figure 3.1: PCR based genotype confirmation of AA, SS, SSCKO mouse models. PCR was performed, and bands were visualized by 1.2% Agarose gel electrophoresis using 100 bp DNA ladder under UV. Panel 1A: Lanes 1,2,3 demonstrate AA genotype containing both normal human α and β globin bands at 320 bp, whereas lanes 4-9 show SS band at 250 bp. Panel 1B (Lanes 2,3) show heterozygous AS mouse genotype bands between 250 and 320 bp; Panel 1C (Lanes 7,8) indicates WT/CKO band at 432 pb; Panel 1D demonstrates the presence of human α globin band at 330 pb; panel 1E (Lanes 2,3,5, and 6) demonstrates the presence of calpain-1 band at 650 bp; panel 1F (Lanes 4,7, and 8) confirms the absence of calpain-1 gene with the Neo Cassette in SSCKO mouse model band at 415 pb;

3.2 Analysis of normoxia and hypoxia data

To investigate whether genetic deletion of calpain-1 regulates RBC morphology of SCD, red blood cells of AA, SS and SSCKO mouse models were exposed to normoxia (20% O_2, T-37ºC) and Hypoxia (3% O_2, 5% CO_2, T-37ºC) at different time points. No sickling was observed in the RBCs and reticulocytes of AA mice under both normoxia and hypoxia conditions. The percent RBC sickling in untreated SS was 9.2% ± 1.95 (± SD), and 8.9% ± 1.93 (± SD) in SSCKO mice. Similarly, no significant differences were

observed between SS and SSCKO reticulocytes at normoxia. The number of sickle reticulocytes in SS was 2.9% ± 0.78% and SSCKO was 2.6%± 1.18% as shown in Figure 3.3 and Figure 3.4, respectively. On the contrary, under hypoxia (3% O_2, 5% CO_2, T-37^oC) for 1 and 2 hours, the percentage of sickle RBCs increased in a time-dependent manner from 10.5%± 2.96 to 17.3%± 2.22 in SS and from 9.6% ± 2.51 to 15.2%± 3.28 in SSCKO without showing a significant difference. Surprisingly, significant differences were observed between SS and SSCKO at 3-hours of hypoxia exposure (Two-way ANOVA, ****P <0.0001, with post-hoc Tukey's test SS vs SSCKO ** p<0.01, N=10). When cell exposure time was increased to 3-hours of hypoxia, the percentage of sickle RBCs in SS was substantially elevated to 27.8%± 3.21, whereas sickling in SSCKO was only increased by 19.9%± 3.17 (Figure 3.6). The percentage of sickle reticulocytes was calculated to be 11.9%± 5.5 in SS and 7.4%± 1.34 in SSCKO at 2-hour hypoxia (post-hoc Tukey's test SS vs SSCKO *p<0.05, N=10); However, when incubation time was increased to 3-hour, the percentage of sickle reticulocytes increased to 34.9%± 5.92 in SS and 26.2%± 2.94 in SSCKO, respectively (Two-way ANOVA, ****P <0.0001, with post-hoc Tukey's test SS vs SSCKO ** p<0.01, N=10) (Figure 3.7). These results show that the SSCKO mice show higher resistance to hypoxia-induced sickling of both RBCs and reticulocytes as compared to SS at 3-hour of hypoxia. Genetic deletion of calpain-1 gene in SS mice may partially rescue the hypoxia-induced RBC/reticulocyte sickling in SCD. Thus, calpain-1 may contribute to the regulation of RBC membrane properties and shape in SCD under certain hypoxic conditions.

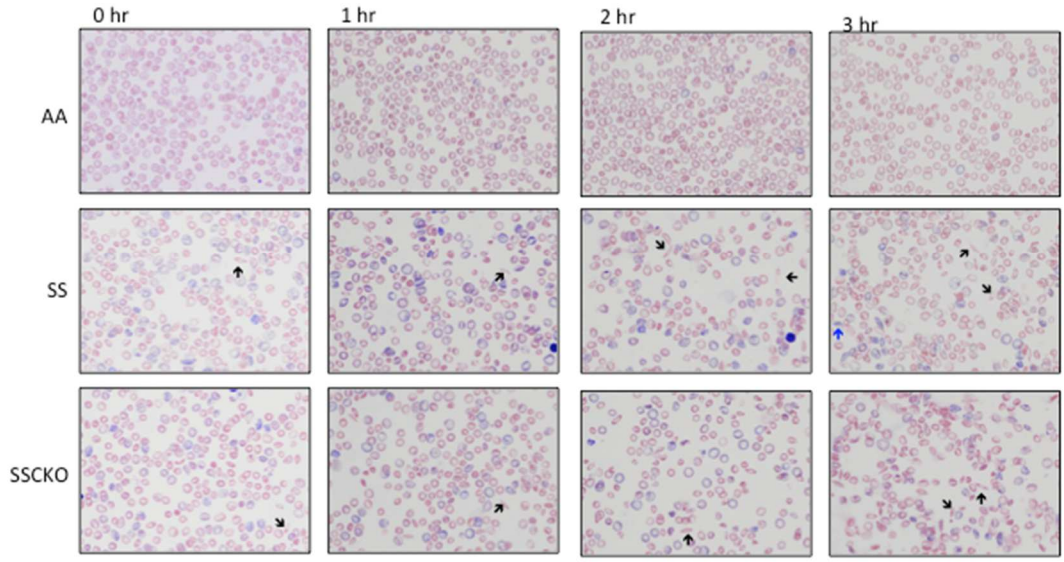

Figure 3.2: Normoxia. Evaluation of AA, SS and SSCKO erythrocyte/reticulocyte morphology by light Microscopy.
Blood was collected from the facial vein of AA, SS and SSCKO mice and incubated under normoxia (20% O_2, T-37^oC) at 1, 2 and 3hour. Blood was smeared on single frosted glass slides. Each slide was fixed with 100% Methanol for 30 seconds and left to dry overnight. Slides were stained with Wright-Giemsa Dye for 30 seconds and washed immediately with water for 10 minutes and air-dried for at least 40 minutes. Slides were examined for cell morphology under 60X objective by a Nikon immersion oil microscope.

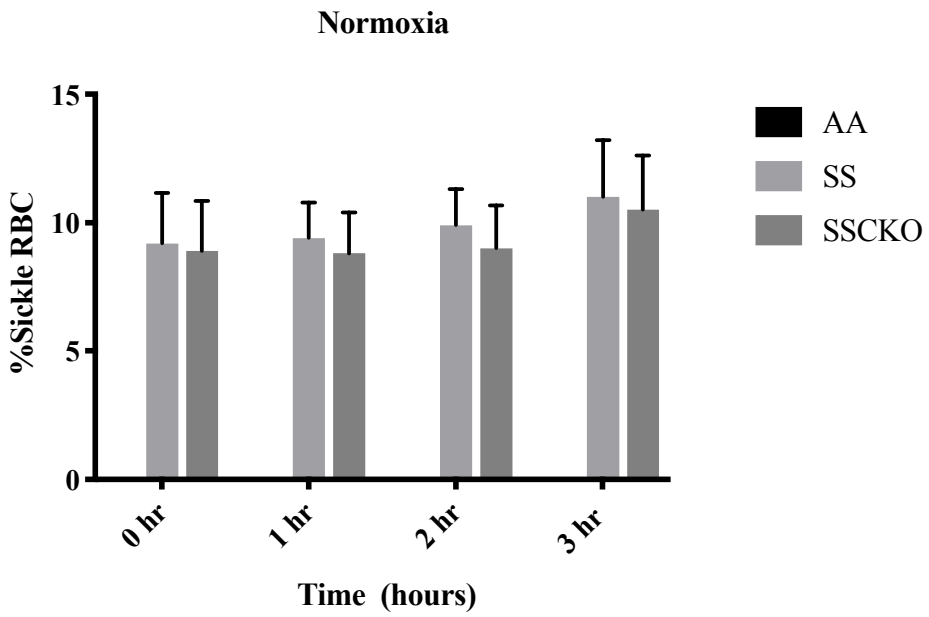

Figure 3.3: Normoxia. Effect of calpain-1gene deletion on sickle erythrocytes.
RBCs from AA, SS and SSCKO mouse models were incubated for 0,1,2, and 3hour under normoxia at 20% O_2, T-37ºC. AA cells did not sickle at all; whereas there was no significant difference was observed between SS and SSCKO groups. Two-way ANOVA, interaction between groups is non-significant.

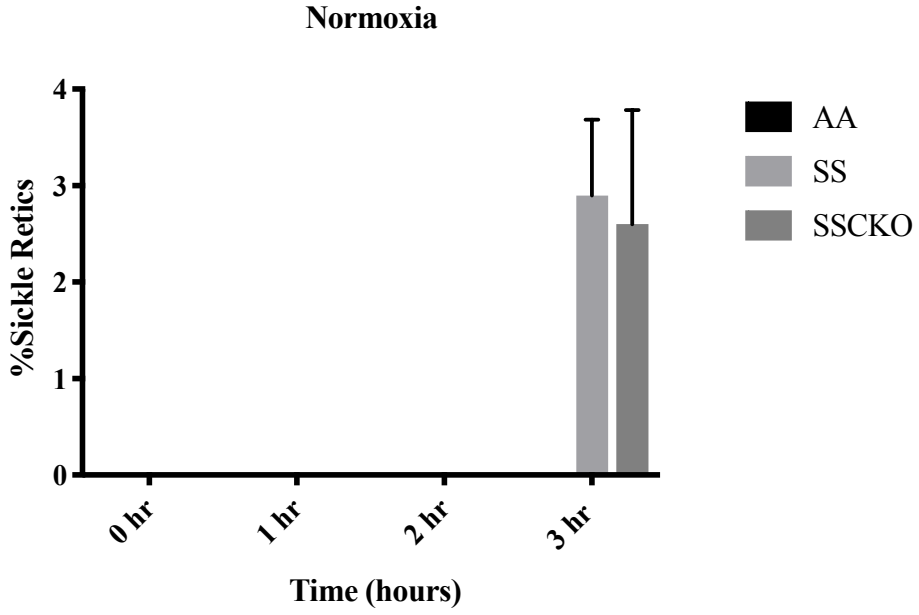

Figure 3.4: Normoxia. Effect of calpain-1 gene deletion on sickle reticulocytes.
No significant difference was observed on sickle reticulocytes between SS and SSCKO Two-way ANOVA, interaction between groups is non-significant.

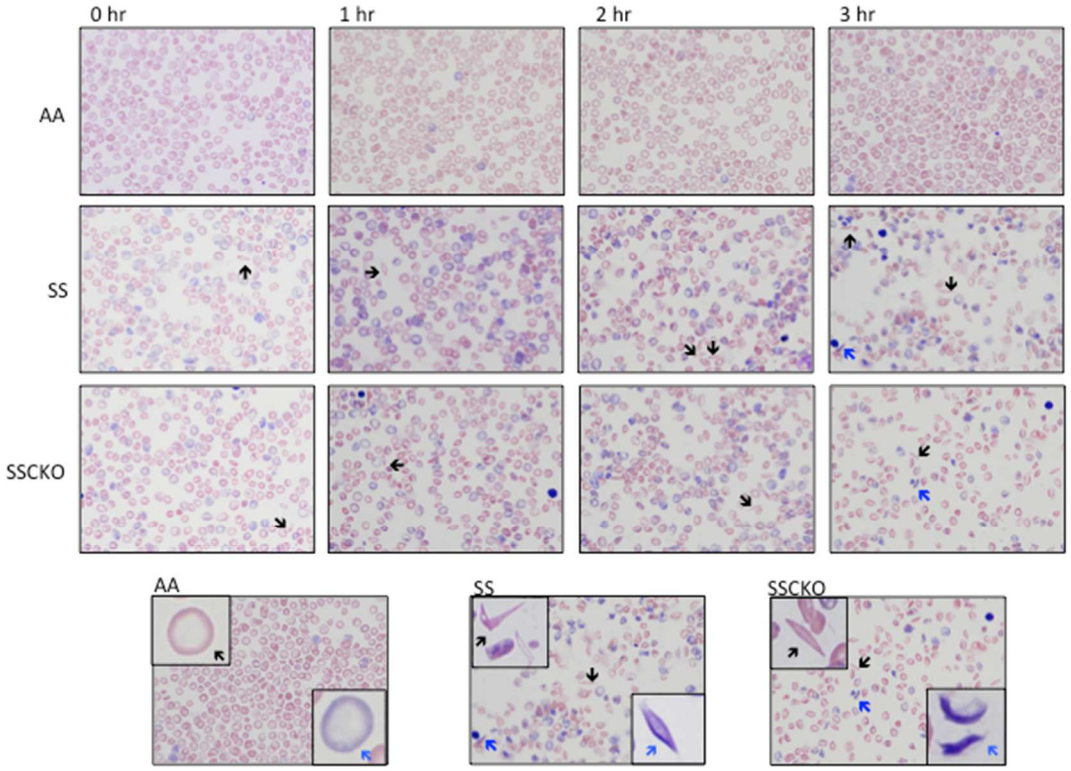

Figure 3.5: Hypoxia. Effect of calpain-1 gene deletion on AA, SS and SSCKO erythrocytes.
Blood was collected from the facial vein of AA, SS and SSCKO mice and exposed under hypoxia (3%O_2, 5% CO_2, T-37^oC) at 1, 2 and 3-hour. Black arrow indicates RBCs and blue arrow shows reticulocytes. Selected images from AA, SS and SSCKO models exposed to 3-hour hypoxia are shown as inset in the lower panels.

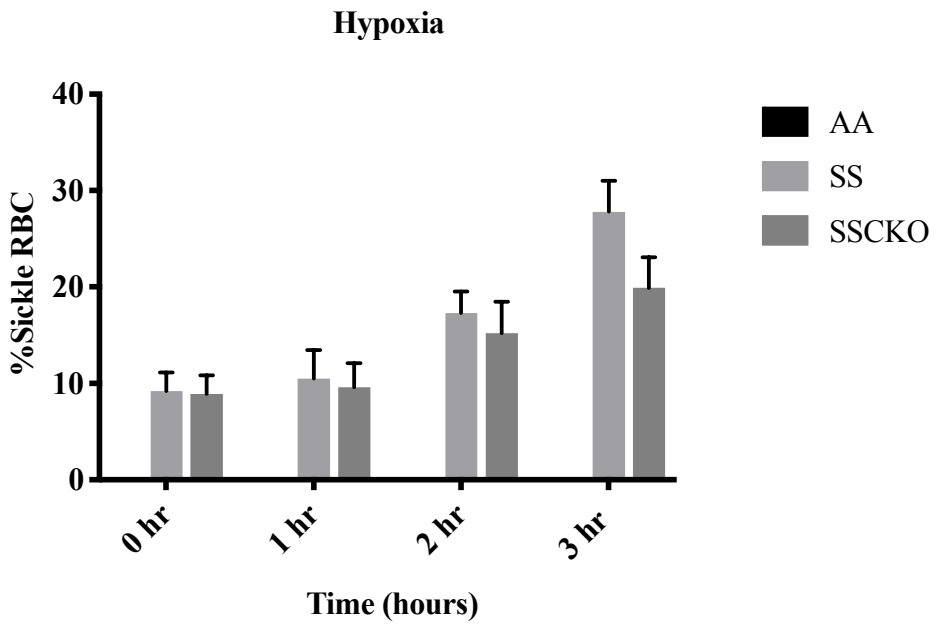

Figure 3.6: Hypoxia. Quantification of sickle erythrocytes under hypoxia.
RBCs of AA, SS and SSCKO were subjected to 0,1,2, and 3-hours of hypoxia under 3% O_2, 5% CO_2, T-37ºC. The AA cells did not sickle at all. There was no significant difference observed between sickle RBCs from SS and SSCKO at 0,1, and 2-hour of hypoxia. However, the percentage of sickle RBCs significantly increased in SS as compared to SSCKO at 3-hour hypoxia (Two-way ANOVA, ****P <0.0001, with post-hoc Tukey's test SS vs SSCKO ** p<0.01, N=10).

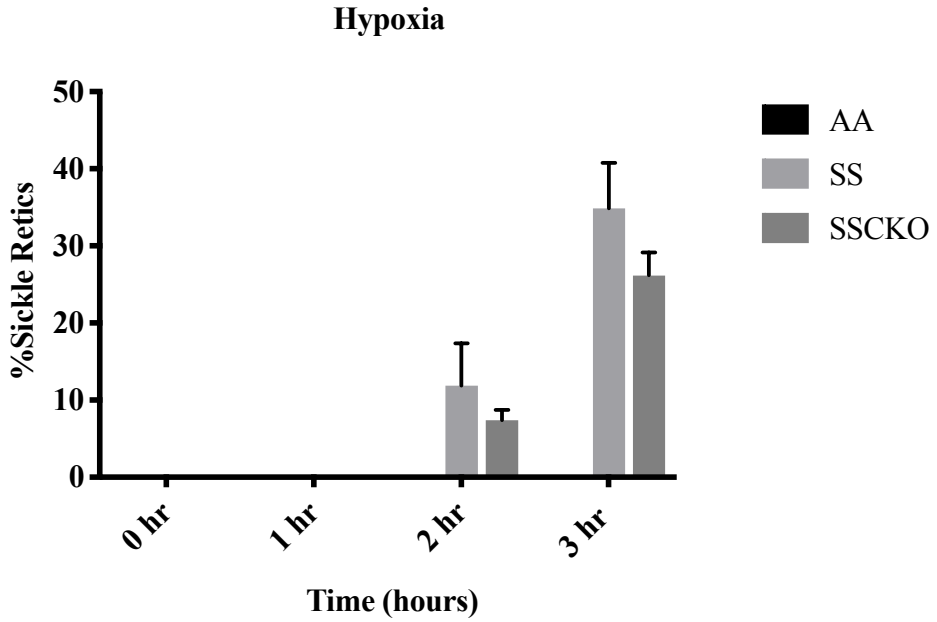

Figure 3.7: Hypoxia. Quantification of sickle reticulocytes under hypoxia.
(Two-way ANOVA, ****P <0.0001, with post-hoc Tukey's test SS vs SSCKO ** p<0.01, N=10).

3.3 Pharmacological inhibition of calpain activity in Sickle erythrocytes/reticulocytes

Unlike erythrocytes, the calpain-2 activity is detectable in reticulocytes (22, 34, 35, 36, 43). Therefore, there is a possibility that calpain-2 might be activated as a compensatory mechanism in SSCKO mice and contribute to sickling process. To investigate this possibility, SS erythrocytes were incubated with and without MDL28170 at two doses of 100 μM and 500 μM dissolved in two different DMSO concentrations of 0.1% and 0.5% under 3-hour hypoxia. MDL28170 is a cysteine protease inhibitor that inhibits both calpain-1 and calpain-2 (29). SS cells treated with MDL28170 at 100 μM with 0.1% DMSO showed a significant reduction in sickle RBCs and reticulocytes. For example, percentage of sickle RBCs declined from 30.1% ± 3.9 to 18.3%± 4.1 (60.7% decrease) and sickle reticulocytes were reduced from 37.9%± 5.13 to 27.4%± 6.92 (72.2% decrease) as shown in Figure 3.9. When the concentration of MDL28170 inhibitor was increased to 500 μM, the percentage of sickle RBCs further reduced from 30.1%± 3.92 to 10.7%± 1.37 (35.5% decrease) and sickle reticulocytes from 39.2%± 5.38 to 14.6%± 2.18 (37.2% decrease). No difference was detectable between untreated and DMSO treated cells as shown in Figure 3.10.

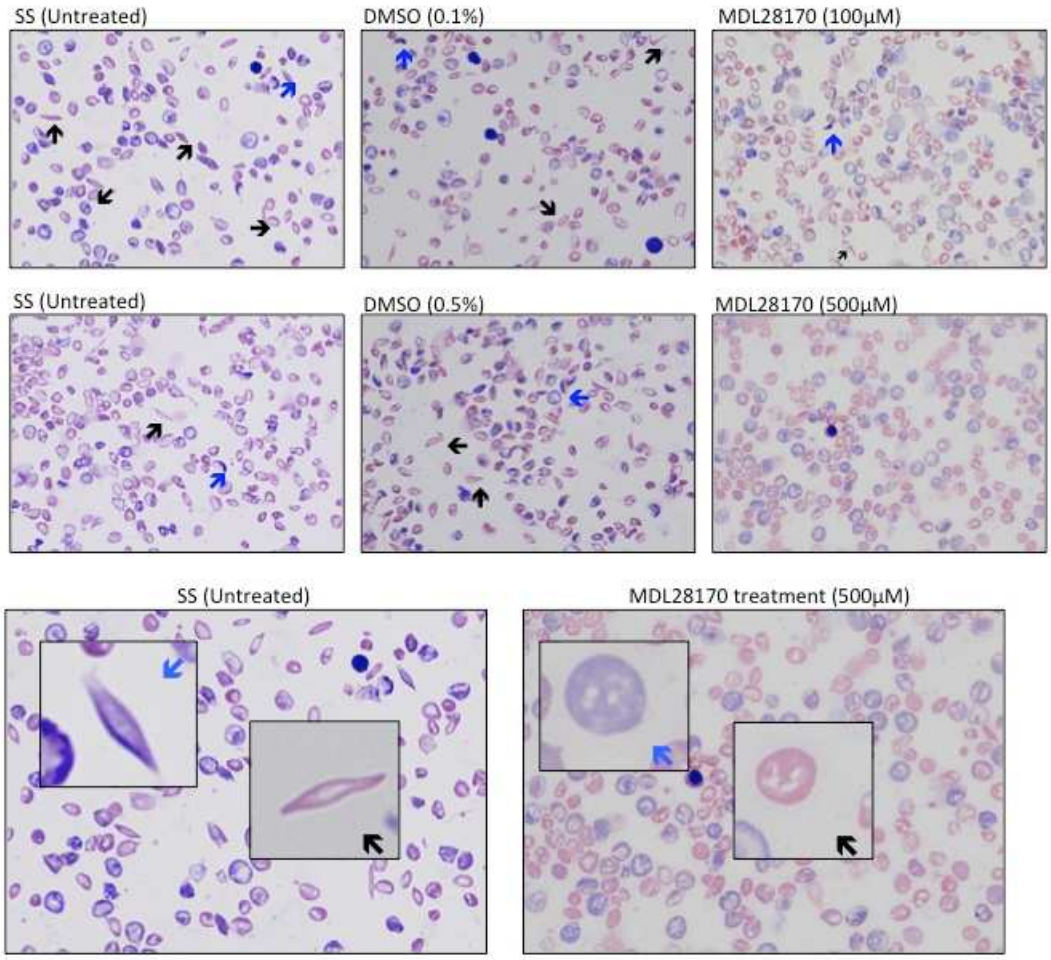

Figure 3.8: Effect of MDL28170 treatment on sickle RBCs and reticulocytes. RBCs isolated from SS model were incubated with and without MDL28170 at concentrations of 100 µM and 500 µM dissolved in two different DMSO concentrations of 0.1% and 0.5% under 3-hour hypoxia (3%O_2, 5% CO_2, T-37ºC). Each sample was smeared, stained, and visualized under 60X objective using a Nikon immersion oil microscope. Black arrows indicate RBCs and blue arrows show reticulocytes. The inset panels show SS cells under 3-hours of hypoxia with and without the treatment of 500 µM MDL28170.

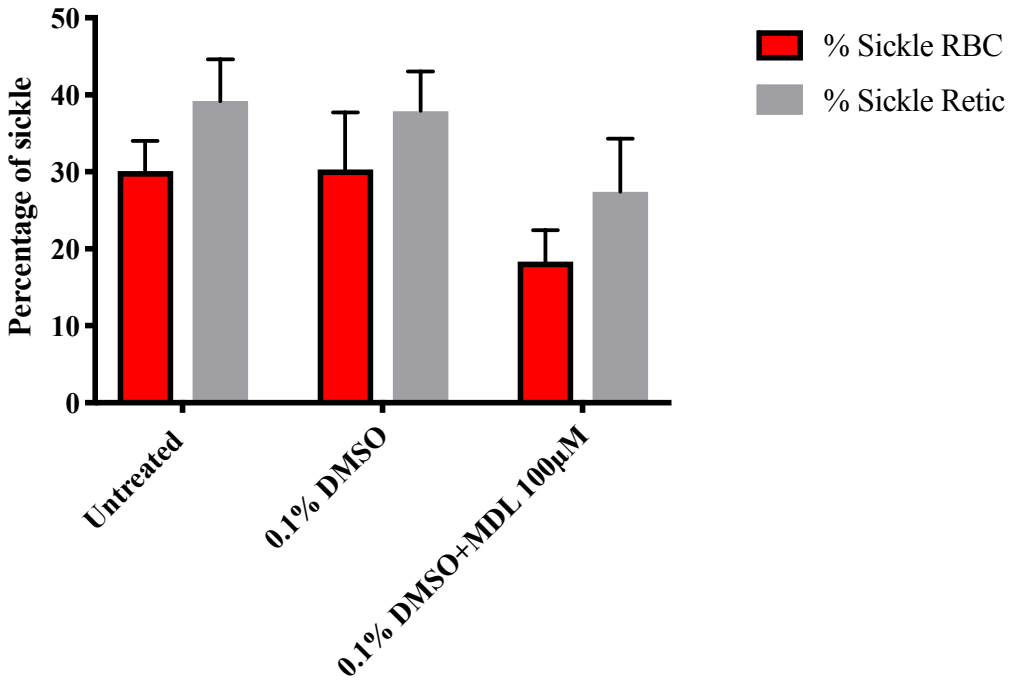

Figure 3.9: Effect of MDL28170 (100 µM) treatment on sickle RBCs and reticulocytes. RBCs from of SS mice were treated with and without MDL28170 at 100 µM concentration in the presence of 0.1% DMSO. The number of sickle RBCs and reticulocytes were counted by microscopy. (Two-way ANOVA, difference between groups ****P <0.0001, with post-hoc Tukey's test, untreated vs 0.1% DMSO insignificant; Untreated vs MDL 100 µM ** p<0.01; 0.1% DMSO vs MDL 100 µM ** p<0.01, N=10).

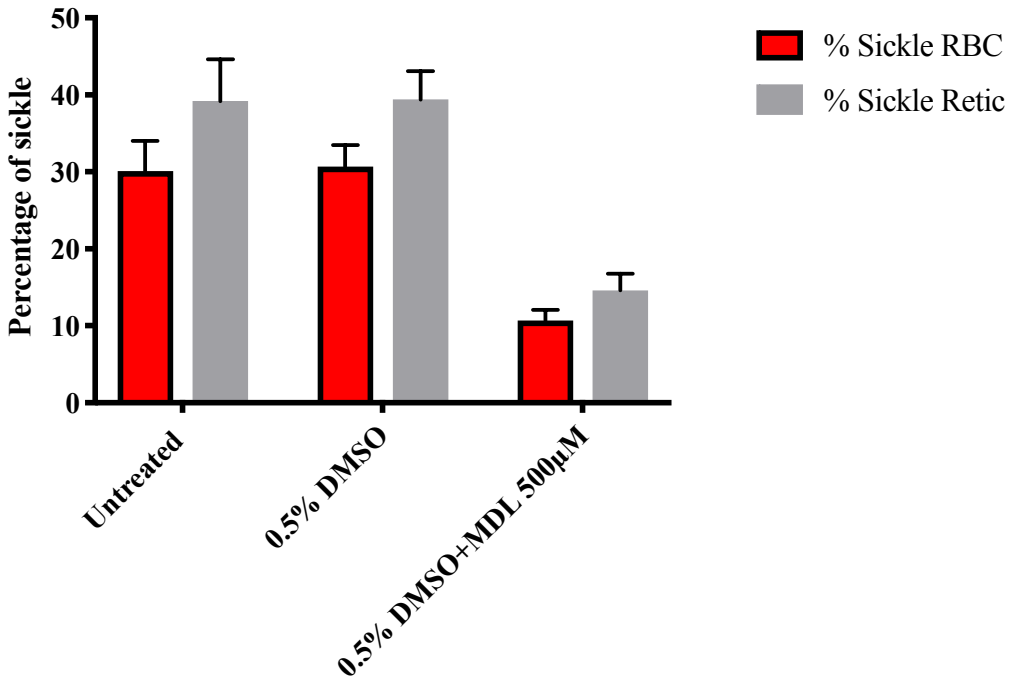

Figure 3.10: Effect of MDL28170 (500 µM) treatment on sickle RBCs and reticulocytes. RBCs from SS mice were treated with calpain inhibitor at 500 µM concentration in the presence of 0.5% DMSO. The number of sickle RBCs and reticulocytes were counted by microscopy. (Two-way ANOVA, difference between groups ****P <0.0001, with post-hoc Tukey's test, untreated vs 0.5% DMSO insignificant; Untreated vs MDL 500 µM ** p<0.01; 0.1% DMSO vs MDL 500 µM ** p<0.01, N=10).

3.4 Measurement of total calpain activity in sickle RBCs/Reticulocytes membranes

The calpain activity was measured in a mixture of RBC and reticulocyte derived plasma membranes (ghosts) using the commercial Calpain Glo Protease Luciferase assay as mentioned earlier. Total calpain activity was determined by measuring the luminescence signal (RLU) in samples harvested from AA, SS and SSCKO mouse models. The results indicate higher calpain activity in SS (8587.4± 2107.4) as compared to AA (7289± 1085.6) and relatively less enzyme activity in the SSCKO (5937.2± 571.3) as shown in Figure 3.11 (Two-way ANOVA, difference between groups *P <0.01; AA vs SS ns, AA vs SSCKO ns; SS vs SSCKO * p<0.05; N=5).

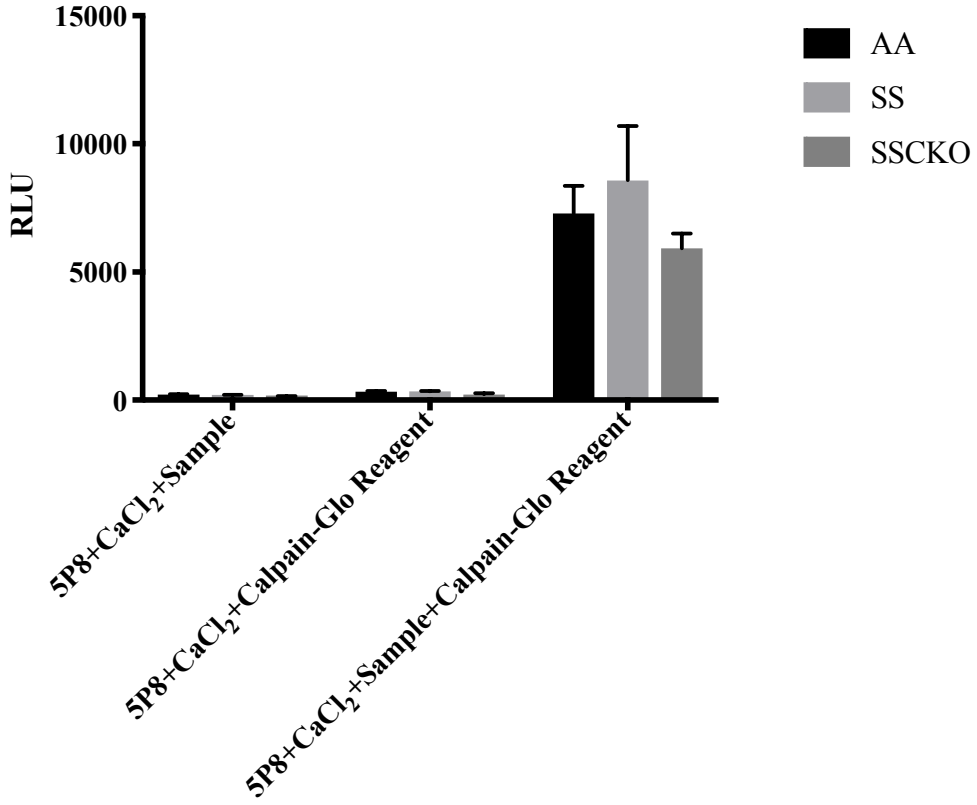

Figure 3.11: Calpain activity measurements in the AA, SS, SSCKO erythrocyte/reticulocyte membranes.
The calpain activity was measured in erythrocyte/reticulocyte ghosts using the Calpain Glo Protease Luciferase assay. Total calpain activity was determined by measuring the luminescence signal (RLU) in the ghosts samples of AA, SS and SSCKO (Two-way ANOVA, difference between groups *P <0.01; AA vs SS ns, AA vs SSCKO ns; SS vs SSCKO * p<0.05; N=5).

3.5 MDL-28170 mediated inhibition of calpain activity in Sickle cell membranes in vitro

To investigate the effect of MDL28170 on total calpain activity in sickle RBC/Reticulocyte membranes (ghosts), the purified ghosts harvested from SS mice were treated with MDL12070 inhibitor at two concentrations at 100 μM and 500 μM in the presence of 0.1% and 0.5% DMSO. As shown in Figure 3.12 and Figure 3.13, inhibitor

treatment markedly reduced calpain activity in the SS ghosts as compared with untreated and DMSO treated membranes. There were no significant differences between the untreated and DMSO treated cells. The calpain activity was reduced from 6114± 78.11 to 1589± 43.15 RLU as shown in Figure 3.13. Interestingly, the reduction of calpain activity was almost similar at both concentrations of inhibitor. The MDL12070 at 100 µM reduced calpain activity to 1754± 47 RLU whereas 500 µM concentration reduced enzyme activity to 1589± 43.15 RLU. These data show that MDL28170 inactivates both calpain-1 and calpain-2 associated with the SS membranes.

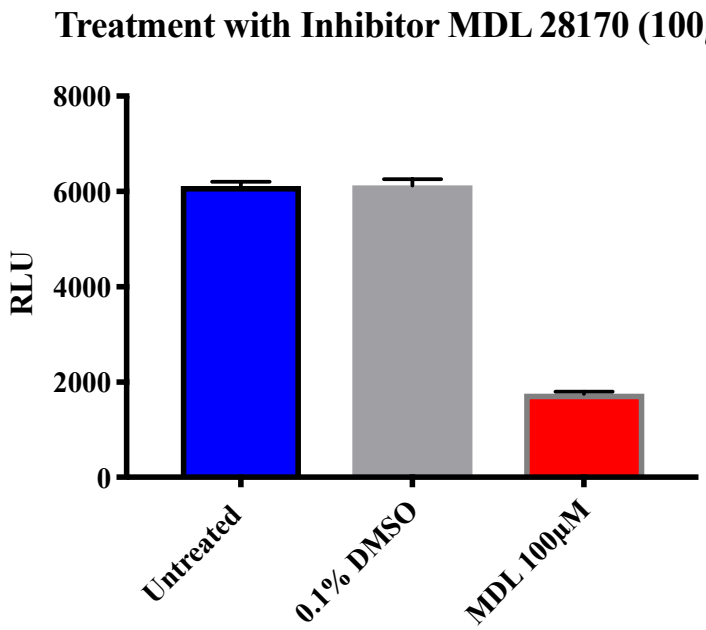

Figure 3.12: Effect of MDL28170 (100 µM) inhibition on SS membranes. RBC/Reticulocyte ghosts harvested from SS mice were treated with calpain inhibitor at a concentration of 100 µM in the presence of 0.1% DMSO (One-way ANOVA, difference between groups ****P <0.0001, with post-hoc Tukey's test, untreated vs MDL 100 µM ** p<0.01; 0.1% DMSO vs MDL 100 µM ** p<0.01. There was no difference between untreated and DMSO treated membrane samples, N=5).

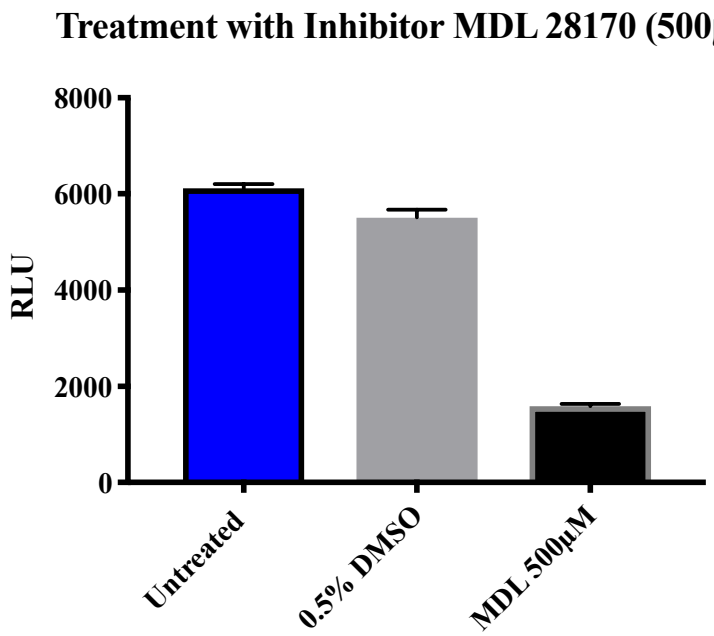

Figure 3.13: Effect of MDL28170 (500 μM) inhibition on SS membranes. RBC/Reticulocyte ghosts harvested from SS mice were treated with calpain inhibitor at a concentration of 500 μM in the presence of 0.5% DMSO (One-way ANOVA, difference between groups ****P <0.0001, with post-hoc Tukey's test, untreated vs MDL 500 μM ** p<0.01; 0.5% DMSO vs MDL 500 μM ** p<0.01. There was no differences between untreated and DMSO treated membrane samples, N=5).

3.6 Normalization of protein concentration by Bradford assay

Protein concentrations were measured in the ghosts of AA, SS and SSCKO at 595nm absorbance using the microplate reader. A standard curve was generated by seven serial dilutions of protein (125 μg/ml BSA) and protein concentration was calculated based on the standard curve. The AA sample corresponds to 54 μg/ml, SS sample corresponds to 58 μg/ml, and SSCKO sample corresponds to 60 μg/ml as shown in Figure 3.14.

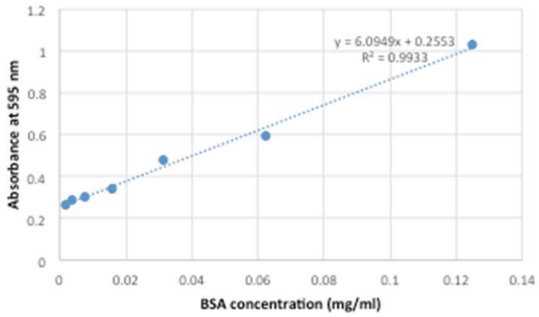

Figure 3.14: Protein quantification by Bradford assay.
A standard protein curve was generated by measuring absorbance at 595 nm (BSA 125 µg/ml). Protein concentration ranged between 20 to 140 µg/ml.

3.7 Western blot analysis of calpain-1

Western blot analysis was performed to assess the status of membrane-associated calpain-1 protein in AA, SS and SSCKO samples using a calpain-1 monoclonal antibody. The antibody detected a comparable intensity of 80-kDa protein band in AA and SS samples, whereas the SSCKO did not show any detectable calpain-1 band (Figure 3.15). These results confirm the absence ofcalpain-1 gene in SSCKO mice. It is to be noted that heating of the membrane protein samples at 90^{o}C for 5 minutes degraded the calpain-1 protein in the SS sample but not in the AA sample (Figure 3.16). Therefore, all samples were loaded without heating.

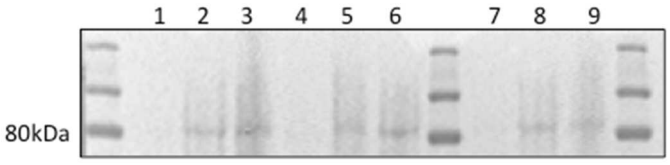

Figure 3.15: Western blot analysis of calpain-1 in AA, SS, and SSCKO ghosts.
SDS/PAGE of RBC/reticulocyte ghosts isolated from AA, SS, and SSCKO. No detectable band of calpain-1 at 80 kDa was observed in SSCKO as shown in lanes 1, 4, 7. Lanes 2, 5, and 8 show membrane samples from SS and lanes 3, 6, and 9 show protein samples from AA mice.

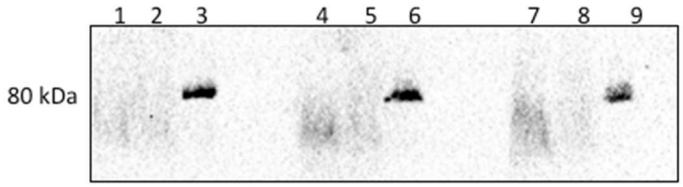

Figure 3.16: Western blot analysis of calpain-1 in AA, SS, and SSCKO ghosts. SDS/PAGE of RBC/reticulocyte ghosts isolated from AA, SS, and SSCKO. Lanes 3, 6, and 9 show an intense 80-kDa band in the AA sample. The 80kDa band disappeared in the SS upon heating of the sample at 90^{o}C for 5 minutes as shown in lanes 2, 5, and 8. No band was observed in the SSCKO sample as shown in lanes 1, 4, and 7.

Chapter 4: Discussion and Conclusions

The purpose of this study was to investigate the functional role of erythrocyte calpain-1 in sickle cell disease (SCD) using a calpain-1 null mouse model of SCD. In this study, intact RBCs and reticulocytes harvested from AA, SS and SSCKO mice were exposed to normoxia (20%- O_2, T-37^oC) and hypoxia (3%- O_2, 5%- CO_2, T-37^oC) at different time points. No measurable differences were observed between the three groups under normoxia condition. However, SSCKO showed significant resistance to hypoxia-induced sickling as compared to SS upon 3-hour exposure to hypoxia (Figure 3.6. and 3.7). The difference between the SS and SSCKO is significant (post-hoc Tukey's test SS vs SSCKO ** $p<0.01$, N=10). These findings demonstrate that sickling of RBCs and reticulocytes is time-dependent. When the incubation time of cells under hypoxia was increased, the number of sickle RBCs and reticulocytes were also proportionally increased in a time-dependent manner. Surprisingly, the reticulocytes did not sickle at the baseline normoxia, and required relatively longer incubation time to sickle under these conditions. One possibility is that reticulocytes containing both calpain-1 and residual level of calpain-2 might not sickle at physiological condition and require relatively higher hypoxic stress to activate calpain-2 for optimum sickling.

It is known that calcium-dependent K channels are not activated in oxygenated sickle RBCs (13, 17) and it has been reported that reticulocytes are permeable to calcium only under deoxygenation conditions (17). The oxygenated sickle RBCs show a modest enhancement (50%) of permeability to external calcium, and deoxygenation boosts the calcium influx by approximately fivefold (17). Our laboratory has shown previously that activation of Gardos channel in SCD is suppressed by the deletion of calpain-1 gene (23).

Similarly, pharmacological inhibition of calpain-1 by BDA-410 *in vivo* prevented hypoxia-induced RBC dehydration in a mouse model of mild SCD (22, 23). Human SS erythrocytes contain approximately eight times higher calcium concentration as compared to normal erythrocytes (13), and their permeability to calcium increases dramatically upon deoxygenation thus triggering Hb polymerization and enhanced sickling (13).

Since calpains are calcium activated cysteine proteases (22), it is likely that they contribute to the sickling process upon elevation of calcium in SCD under hypoxic conditions. This model is consistent with the evidence indicating a connection between human SS erythrocytes and an abnormal accumulation of intracellular calcium activating calpain-1 under hypoxic stress (13, 34). Moreover, prior studies from our laboratory (22, 23) and others (19, 27) have demonstrated that the cellular dehydration under deoxygenated state may trigger excessive accumulation of intracellular calcium with concomitant activation of calpain-1 in the RBC membrane. These studies suggest that a causal relationship may exist between calpain-1 activation, elevated sickling, and higher crisis rates that are observed in patients with less dehydrated and more deformable erythrocytes.

It is noteworthy that Townes SS mice carry >50% reticulocytes in their peripheral circulation under steady state conditions of normoxia (20, 35). This issue is relevant to the calpain biology since mature erythrocytes only express calpain-1 whereas reticulocytes express both calpain-1 and calpain-2. The calpain-2 activity in reticulocytes is approximately 5-10% of the total cysteine protease activity. This differential expression of calpain-1 and calpain-2 in erythrocytes and reticulocytes raises the

possibility that systemic inactivation of calpain-1 gene in SSCKO mice may induce a compensatory increase of residual calpain-2 in reticulocytes. Consistent with our previous findings (15, 35, 43), our calpain activity measurements indicate that calpain-2 enzyme is not upregulated in SSCKO reticulocytes. Nonetheless, the presence of residual calpain-2 in reticulocytes can in principle lead to a differential response for pharmacological inhibition of calpain activity in SS erythrocytes and reticulocytes. This hypothesis seems to be consistent with our findings showing a differential effect of MDL28170, a pan-calpain inhibitor, on the sickling properties of erythrocytes and reticulocytes. When SS cells (both erythrocytes and reticulocytes) were treated with 100 μM MDL28170 under 3-hour hypoxia, the calpain inhibitor significantly reduced the sickling propensity of both erythrocytes and reticulocytes. Interestingly, the percentage of RBC sickling at 100 μM dose declined from 30.1% to 18.3% (60.7% decrease), and sickle reticulocytes were reduced from 37.9% to 27.4% (72.2% decrease) as shown in Figure 3.9. When the inhibitor concentration was increased to 500 μM, the percent decrease in sickling was further reduced to 10.7% (35.5% decrease) for erythrocytes and 14.6% (37.2% decrease) for reticulocytes (Fig 3.10). Similarly, the calpain activity was also decreased in SSCKO compared to SS with similar inhibition at different dose concentration of calpain inhibitor MDL28170. Our previous studies using casein zymography have confirmed the absence of calpain-1 enzymatic activity in the erythrocytes and reticulocytes of SSCKO mice as compared to Hb AA-Townes and Hb SS – Townes sickle mice (35, 36).

There have been numerous studies investigating the therapeutic effects of MDL28170 on different cell types (37, 29). In this study, we elected to investigate the

role of calpain activity in the erythrocyte membrane since the biochemical abnormalities in SCD occur mainly in the plasma membrane upon deoxygenation of sickle hemoglobin (19, 22, 27). The correlation between increased intracellular calcium and activation of calpain-1 in erythrocytes and reticulocytes are likely to contribute to the regulation of sickle shape of RBCs further exacerbating the vaso-occlusive events during microcirculation.

There is considerable interest in the elevation of fetal hemoglobin (HbF) as a potential therapeutic option to reduce sickling and associated pathologies in sickle cell disease (12, 20). It is now well established that elevation of fetal hemoglobin (HbF) by more than 20% is sufficient to reduce the deleterious lesions including the painful crisis episodes in SCD patients (19, 27). In contrast to the accepted model of reducing sickling by elevating HbF, here we provide evidence for a novel strategy of reducing sickling under hypoxia that is independent of its effect on HbF for the following reasons. First, we used adult mice aged between 5-10 months, which do not show any therapeutic elevation of HbF at this age. The newborn sickle mice express high levels of HbF (~30-50%) that declines by one month to HbS (20). In the normal adult mice, the HbF is expressed approximately at 3.2-7.7%. Similarly, adult homozygous sickle (HbSS) patients carry approximately 5.8% HbF with variation ranging from 0.5% and 18.8% (20). Second, the HPLC based measurements of globin chains in transgenic sickle mice show that HbF is not elevated in adult sickle mice (20, 42). These observations support the current paradigm that both adult sickle patients and mice do not express any therapeutic levels of fetal hemoglobin *in vivo*. The experiments reported in this Thesis were performed on erythrocytes and reticulocytes that were harvested from adult sickle mice.

Moreover, the observed phenotype of reduced sickling was detected when adult sickle cells were treated with a calpain inhibitor for 3-hours under hypoxia. Therefore, it is highly unlikely that there would be any elevation of fetal hemoglobin upon 3-hours of hypoxia exposure when the cells did not contain at elevated HbF under baseline normoxia conditions. In any case, future studies may be necessary to quantify the level of HbF in SS mice exposed to hypoxia while undergoing therapeutic correction of sickling by pharmacological calpain inhibitors.

In conclusion, our findings are consistent with the previous studies showing a functional role of calpain activity in the remodeling of the erythrocyte membrane and cell shape (22,23,34). Both genetic deletion of calpain-1 in SS mice and pharmacologic inhibition of calpain activity reduces erythrocyte and reticulocyte sickling presumably by restoring the morphology and membrane properties of sickle cells *in vivo* and *in vitro*. While the future studies will continue to refine the precise mechanisms of calpain-mediated remodeling in erythrocytes, there is adequate experimental evidence now available to warrant further testing of synthetic pharmacological inhibitors as potential therapeutic anti-sickling compounds. The strategy proposed here may unveil a novel fetal hemoglobin independent modality to treat sickling and associated lesions in patients with sickle cell disease.

Chapter 5: References

1. Dong, C., Chadwick, R. S., & Alan N. Schechter, A. N. (1992). Influence of sickle hemoglobin polymerization and membrane properties on deformability of sickle erythrocytes in the microcirculation. *Biophysical Journal, 63*, 774-783.
2. Melloni, E., & Pontremoli, S. (1991). The calpain-calpastatin system: structural and functional properties. The Journal of Nutritional Biochemistry, 2(9), 467-476.
3. Nikkel, A.L., Martino, B., Markosyan, S., Brederson, J., Medeiros, R., Moeller, A., & Bitner, R.S. The novel calpain inhibitor A-705253 prevents stress-induced tau hyperphosphorylation in vitro and in vivo. (2012) *Neuropharmacology,*63, 606-612
4. Li, X., Chen, H., Jeong, J & Chishti, A. (2007). BDA-410: A novel synthetic calpain inhibitor active against blood stage malaria. *Molecular & Biochemical Parasitology, 155,*26–32
5. Sandmann, S., Prenzel, F., Shaw, L., Schauer, R & Unger, T. (2002). Activity profile of calpains I and II in chronically infarcted rat myocardium influence of the calpain inhibitor CAL 9961. *British Journal of Pharmacology*, 135, 1951-1958.
6. Abbyad, A., Tharaux, P., Martin, J., Baroud, C., & Alexandrou, A. Sickling of red blood cells through rapid oxygen exchange in microfluidic drops. (2010). *Lab Chip, 10,* 2505–2512. DOI: 10.1039/c004390g
7. Call, D. E., Thompson, V., Wei, H., & C, J. The Calpain System. (2003). *Physiological review, 83*, 731–801.
8. Kaul, D., & Xue, H. (1991). Rate of deoxygenation and rheologic behavior of blood in sickle cell anemia. *Blood, 77*(6), 1353-1361.
9. Beers, E. J., Samsel, L., Mendelsohn, L., &. Kato, G. (2014).· Imaging flow cytometry for automated detection of hypoxia- induced erythrocyte shape change in sickle cell disease. *American Journal of Hematology, 89*(6), 598–603.
10. Sorimachi, H., Hata, S., & Ono, Y. Impact of genetic insights into calpain biology. (2011). *The Journal of Biochemistry, 150*(1):23–37 doi:10.1093/jb/mvr070
11. Amini, M., Farazifard, R., Zhu, G., Zhang, Y., & Park, D. (2013). Conditional Disruption of Calpain in the CNS Alters Dendrite Morphology, Impairs LTP, and Promotes Neuronal Survival following Injury. *The Journal of Neuroscience*, 33(13), 5773–5784.
12. Xu et al. Correction of Sickle Cell Disease in Adult Mice by Interference with Fetal Hemoglobin Silencing. (2011). *Science*, 334(6058), 993–996. doi:10.1126/science.1211053
13. Eaton. J.W. et al. (1973). Elevated Erythrocyte Calcium in Sickle Cell Disease. *Nature, 246*, 105–106.
14. Steinberg, M. H, et al. (2014). Fetal hemoglobin in sickle cell anemia: a glass half full? *Blood, 123*(4).
15. Azam et al. (2001). Disruption of the Mouse -Calpain Gene Reveals an Essential Role in Platelet Function. *Molecular and Cellular Biology, 21* (6), 2213–2220.

16. Li, X., et al. (2017). Patient-specific modeling of individual sickle cell behavior under transient hypoxia. *PLOS, 13*(3).
17. Hebbel, R. P. (1991). Beyond Hemoglobin Polymerization: The Red Blood Cell Membrane and Sickle Disease Pathophysiology. *Blood,* 77(2), 214-237.
18. Nabeshima, Y at al. (2014). Calpain 1 inhibitor BDA-410 ameliorates a-klotho-deficiency phenotypes resembling human aging-related syndromes. *Sccientific reports, 4* (5847), doi: 10.1038/srep05847.
19. Lande, W.M. et al. (1988). The incidence of painful crisis in homozygous sickle cell disease: correlation with red cell deformability. *Blood, 72*(6), 056-9.
20. Ryan, T.M. et al. (1997). Knockout-transgenic mouse model of sickle cell disease. *Science, 278(*5339), 873-6.
21. Xu, J et al. (2011). Correction of sickle cell disease in adult mice by interference with fetal hemoglobin silencing. *Science, 334*(6058), 993-6. doi:10.1126/science.1211053.
22. Wieschhaus, A.et al. (2012). Calpain-1 knockout reveals broad effects on erythrocyte deformability and physiology. *Biochemical journal, 448*(1), 141-52. doi: 10.1042/BJ20121008
23. De Franceschi, L. et al. (2013). Pharmacological inhibition of calpain-1 prevents red cell dehydration and reduces Gardos channel activity in a mouse model of sickle cell disease.*FASEB Journal, 27*(2), 750-9. doi: 10.1096/fj.12-217836.
24. Ganz, T. (2018). Erythrocytes and erythroblasts give up iron. *Blood, 132*(19), 2004-2005. doi: 10.1182/blood-2018-09-876102.
25. Oliver, W.T. (2018). The effects of Capn1 gene inactivation on the differential expression of genes in skeletal muscle. *Gene, 668*, 54-58. doi: 10.1016/j.gene.2018.05.040.
26. MacLeod, J.A et al. (2018). Genetic disruption of calpain-1 and calpain-2 attenuates tumorigenesis in mouse models of HER2+ breast cancer and sensitizes cancer cells to doxorubicin and lapatinib.*Oncotarget, 9*(70), 33382-33395. doi: 10.18632/oncotarget.26078
27. Du, E. et al. (2015). Kinetics of sickle cell biorheology and implications for painful vasoocclusive crisis. *PNAS, 112* (5) 1422-1427.
28. Sun, K., & Xia, Y. (2013). New insights into sickle cell disease: a disease of hypoxia. *Current Opinion Hematology, 20*(3), 215-21. doi: 10.1097/MOH.0b013e32835f55f9.
29. Ono, Y. et al. (2016). Calpain research for drug discovery: challenges and potential. *Nature Reviews Drug Discovery*, *15*(12), 854-876. doi: 10.1038/nrd.2016.212.
30. Gutsaeva, D.R. et al. (2011). Inhibition of cell adhesion by anti-P-selectin aptamer: a new potential therapeutic agent for sickle cell disease. *Bood, 117*(2), 727-35. doi: 10.1182/blood-2010-05-285718
31. Gutsaeva, D.R. et al. (2014). Molecular mechanisms underlying synergistic adhesion of sickle red blood cells by hypoxia and low nitric oxide bioavailability. *Blood, 123(*12), 1917–1926.

32. Zhang, Y. et al. (2018). Metformin induces FOXO3-dependent fetal hemoglobin production in human primary erythroid cells. *Blood, 132*(3), 321-333. doi:10.1182/blood-2017-11-814335
33. Kling, A.et al. (2017). Discovery of Novel and Highly Selective Inhibitors of Calpain for the Treatment of Alzheimer's Disease: 2-(3-Phenyl-1*H*-pyrazol-1-yl)-nicotinamides. *Journal of Medicinal Chemistry, 60* (16), 7123–7138.
34. Glazer, T., Schwarz-Benmeir, N., Barnoy, S., Barak, S., Eshhar, Z., & Kosower, N. S. (1994). Calpain (Ca^{2+} – dependent thiol protease) in erythrocytes of young and old individuals. *Cell Biology, 91*, 7879-7883.
35. Nwankwo, J. O., Lei, J., Rivera, A., Gupta, K., & Chishti, A. H. (2016). Genetic Inactivation of calpain-1 attenuates pain sensitivity in a humanized mouse model of sickle cell disease. *Haematologica*; doi:10.3324/haematol.2016.148106
36. Nwankwo, J. O., Gremmel, T., Gerrits, A. J., Mithila, F. J., Warburton, R. R., Hill, N. S., & Chishti, A. H. (2017). Calpain-1 regulates platelet function in a humanized mouse model of sickle cell disease. *Thrombosis Research, 160*, 58-65.
37. Tao, X., Shi, J., Hao, S., Chen, X., & Liu, B. (2017). Protective effects of calpain inhibition on Neurovascular unit injury through downregulating nuclear factor-kB- related inflammation during traumatic brain injury in mice. *Chinese Medical journal, 130*(2), 187-98.
38. Yi, X., Liu, M., Zhuo, H., Cao, H., Wang, J., & Han, Y. (2017). Toxic effects of dimethyl sulfoxide on red blood cells, platelets, and vascular endothelial cells in vitro. *FEBS Open Bio, 7,* 485-494.
39. De Bruijne, A. W., & Van Steveninck, J. (1974). The influence of dimethylsulfoxide on the red cell membrane. *Biochemical Pharmacology, 23,* 3247-3258.
40. Tsujinaka, T., Kajiwara, Y., Kambayashi, J., Sakon, M., & Mori, T. (1988). Synthesis of a new penetrating calpain inhibitor (calpeptin*). Biochemical and Biophysical research Communication, 153*(3), 1201-1208.
41. Mehdi, S., Angelastro, M., Wiseman, J., & Bey, P. (1988). Inhibition of the proteolysis of rat erythrocyte membrane proteins by a synthetic inhibitor of calpain. *Biochemical and Biophysical research Communication, 157*(3),1117-1123.
42. Paszty, C., Brion, C., Manci, E., & Rubin, E. (1997). Transgenic knockout mice with exclusive human sickle hemoglobin and sickle cell disease. *Science, 278*(5339), 873-876.
43. Nwankwo, J. O., Huang, S., Han, J., & Chishti, A. (2014). Genetic deletion of calpain-1 improves reticulocyte deformability in a mouse model of sever sickle cell disease. *Blood,124 (21),* 2698.